

A Study of Skin Thermal Responds of Tonification And Sedation In Moxibustion Using A Mathematical Method

Miao Liu (✉ liumiao@sues.edu.cn)

Shanghai University of Engineering Science <https://orcid.org/0000-0001-9762-9523>

S.K. Kauh

Seoul National University

Sabina Lim

Kyung Hee University

Research

Keywords: direct moxibustion, mathematical method, tonification, sedation, skin thermal respond

Posted Date: September 22nd, 2021

DOI: <https://doi.org/10.21203/rs.3.rs-903359/v1>

License:  This work is licensed under a Creative Commons Attribution 4.0 International License.

[Read Full License](#)

Abstract

Background: To research the thermomechanical behavior of skin tissue in tonification and sedation of direct moxibustion.

Methods: A mathematical method was used to study the thermal responses by skin tissue to tonification and sedation of direct moxibustion. Using a standardized method to measure the temperature of a burning barley (*Hordeum vulgare* var.) moxa cone, the temperature, burn damage, and thermal stress distributions in the skin tissue were analyzed.

Results: According to the ideal skin layers and properties of skin-tissue layers, as well as one measured data, the distribution values of temperature, damage, and stress in the skin tissue with respect to tonification and sedation of direct moxibustion was demonstrated.

Conclusion: The thermal responds generated by sedation of direct moxibustion is much larger than those by tonification of direct moxibustion.

Background

Moxibustion is a traditional medicine therapy, and direct moxibustion is one of moxibustion that involves burning moxa or mugwort (*Artemisia vulgaris*) ground to fluff on the skin over an acupuncture point, as shown as Fig. 1. It was developed gradually as early as the discovery and use of fire, and has been used throughout Asia for thousands of years. Up to now, it still plays a significant position in traditional medical systems of China, Japan, Korea, Vietnam, Tibet and Mongolia [1, 2].

Moxibustion is two approaches of moxibustion treatment proposed by Chinese ancestors: tonification and sedation. These approaches are described in the classical book *Miraculous Pivot of The Yellow Emperor's Internal Classic—Ling Shu* (*Miraculous Pivot*, also known as *Canon of Acupuncture*). Tonification is used for reinforcement and involves allowing a slow burning cone to burn out by itself; although the heat is weak, it is persistent and substantial. If this supplementing technique is used, the moxa cone is left alone after it is ignited. It must be allowed to burn gradually and eventually burn out. Then the point is pressed with the hand to make the warming persistent. Sedation is used for reduction. The process involves blowing on the moxa cone. Although the heat is intense, it is temporary and short. If this drainage technique is used, the ignited moxa must be blown upon to increase its speed of burning; then, it either burns out or is removed when it becomes too hot. Unlike tonification, the point is not pressed [3, 4].

In addition, new technical methods, such as new infrared-moxa or laser-moxa devices, electrobian stone moxibustion, and the investigation of a new needle-moxa system using high-technology methods such as thermography, laser Doppler flowmetry, and laser doppler imaging have also emerged [5]. Therefore, the study of the thermomechanical behavior of skin tissue in moxibustion is important.

Barley (*Hordeum vulgare* var.) moxa cone is a small moxa cone that is widely used in scarring moxibustion. When a moxa cone is burned, high-temperature–induced heat energy and chemical substances have significant therapeutic effects, such as treating disease and enhancing health by stimulating blood circulation and improving organ function. Therefore, it is very important analyze the thermomechanical behavior of tonification and sedation to improve treatment effects [6]. However, current temperature measurement technology can only make measurements at fixed points; thus, a mathematical method was used to study the thermomechanical characteristics of scarring moxibustion.

In this paper, we first provide a standardized method to measure the temperature of a burning moxa cone. Second, introduce the mathematical method. Finally, based on the temperature of the burning moxa cone, the results of skin thermal responds about tonification and sedation are presented using a mathematical method.

Temperature measurement

To study the thermal responds of tonification and sedation in moxibustion, the temperature of burning barley moxa should be measured, which is a small moxa cone that is widely used in moxibustion. The burning scope and temperature curve of moxa can be acquired from ideal and standardized burning experiments on barley.

To measure the burning temperature of a moxa cone, we used experimental equipment with a hot plate managed by a control system inside the chamber.

Materials

To test this equipment, we used “KangHwa” moxa made by Ehwadang in the year 2007, and to make the moxa cone for direct moxibustion, we used barley that were produced in Korea. And The properties of the barley moxa cone are shown in Table 1.

The moxa cone was burned on the hot plate in the chamber of this system. The fan and plate temperature were controlled with a microcontroller. A thermocouple was used to link the controller to the ADC (Analog to Digital Converter, 10 bit) switch. Finally, the data were transmitted to the computer. The system is shown in Fig. 2 [7, 8, 9].

Experimental Approach

We used a vernier caliper made by Mitutoyo Co., Japan, with an accuracy of 0.01 mm to measure the size of ten prepared barley moxa cones and ten prepared jujube moxa cones. We also used a Sartorius CP224S scale made by Kinematica AG, Germany, to weigh the 20 prepared samples.

To measure the burning temperature of direct moxibustion, a thermocouple was fixed on a hot plate with a constant temperature of 34°C using aluminum tape. Then a conglutinated barley moxa cone was connected to the thermocouple vertically with saliva. The moxa cone’s apex was lighted with a joss stick.

Then, the temperature of the moxa cone was measured throughout the experiment. A total of 20 samples were prepared. The temperature was measured every second as soon as the moxa cone was lighted. The statistics of the data are shown in Table 1, and Fig. 3.

Table 1
Properties of the Barley Moxa

Common name	Scientific name	Vertical length (mm)	Horizontal length (mm)	Weight of moxa cone (mg)	Peak temperature (F)	Peak time (sec)
Barley moxa	Hordeum vulgare var.	5.3 ± 0.6	3.1 ± 0.2	3.9 ± 1.0	402.2 ± 33.3	11.6 ± 2.6
Note: Each value is mean ± SD;						

Methods

Direct moxibustion requires placing a moxa cone directly on the skin. As the moxa cone burns, the temperature rises on the skin surface; thus, the heat generated on the skin produces thermal responds. To study the thermal response, a finite element method (FEM) analysis of the skin tissue was performed [10].

Skin structure

The skin is the largest multi-layer organ in the body. The structure of skin is extremely complicated, but it is generally made up of four layers: the stratum corneum, the epidermis, the dermis, and the hypodermis, as shown in Fig. 4. In this paper, direct moxibustion bio-thermo-mechanics were studied based on these four layers.

Bioheat transfer

We used the classical, extensively applied Pennes' bioheat equation to describe the heat transfer of direct moxibustion:

$$\rho \frac{\partial T}{\partial t} = k \nabla^2 T + \bar{\omega}_b \rho_b c_b (T_\alpha - T) + q_{met} + q_{ext}$$

1

where ρ is the density of skin tissue; k is the thermal conductivity of skin tissue; $\bar{\omega}_b$ is the blood perfusion rate; ρ_b is the density of blood; c_b is the specific heat of blood; T_α is the temperature of blood; T is the temperature of skin tissue; q_{met} is the metabolic heat generation in the skin tissue; and q_{ext} is the heat generation due to external heating sources [12].

Thermal damage

Currently, the Arrhenius burn integration proposed by Henriques and Moritz [13, 14] is commonly used to describe thermal damage as the following:

$$k(T) = \frac{\partial \Omega}{\partial t} = A \exp\left(-\frac{E_{\alpha}}{RT}\right)$$

2

or equivalently:

$$\Omega = \int_0^t A \exp\left(-\frac{E_{\alpha}}{RT}\right)$$

3

where k is the rate of protein denaturation; t is the exposure time; T is the absolute temperature; A is a material parameter that is equivalent to a frequency factor ($A = 3.1 \times 10^{98}$); E_{α} is the activation energy; and R is the universal gas constant with a value of 8.314 J/mol. K. Our paper uses this concept to analyze thermal damage in skin tissue. Following the method used by Ridge and Wright, the Arrhenius parameters for skin tissue are given by:

$$E_{\alpha} = 21149.324 + 2688.367 \ln(A)$$

4

We calculated the thermal damage value based on the temperature obtained from the bioheat transfer [13, 14, 15].

Note: It is widely accepted that for a first degree burn, $\Omega=0.53$; for a second degree burn, $\Omega=1.0$; and for a third degree burn, $\Omega=10^4$.

Thermal stress

Skin can be considered as a mechanical structure. During moxibustion treatment, the skin experiences mechanical stimulation caused by thermal stress. Here the skin is treated as a laminated composite structure, in which each layer is assumed to be uniform with linear thermo-elastic properties [16].

Mathematical analysis

The finite element method (FEM) is a numerical technique that produces approximate solutions to differential equations that model problems arising in physics and engineering [17]. FEM is now widely used to solve structural, fluid, and multiphysics problems numerically. Furthermore, it is used extensively, because engineers and scientists can model mathematically and solve numerically very complex problems.

Thermal responses of direct moxibustion in skin tissue comprise a multiphysics problem, and hence, the FEM method was used. The exact geometry, the boundary, and initial conditions for the FEM can be given as follows below.

The skin is divided into four layers as mentioned above. Here we used an ideal skin layer, as shown in Fig. 5. Each layer has a different thickness: the thickness of the stratum corneum is 0.02 mm, the thickness of the epidermis is 0.08 mm, the thickness of the dermis is 1.5 mm, and the thickness of the subcutaneous fat is 4.4 mm. While blood perfusion only occurs in the dermis layer, metabolic heat generation occurs in all four layers [18].

According to the skin structure, it is known that many types of diversified sensor cells are distributed in the dermis layer. Thus, our experiment focused on this layer to analyze the biothermomechanics of the epidermis-dermis interface (ED interface).

Based on the temperature measurement of barley moxa cones, the statistics of the data are shown in Table 1, which were selected as heat resource data for the thermomechanics analysis.

To compute the skin thermal responds of tonification and sedation in moxibustion using the FEM, the parameter values of each skin layer are needed and for the blood, as shown in Tables 2 and 3.

Skin tissue is a complicated multilayer, and the parameters of each layer are used in the formula mentioned earlier and are calculated by FEM. The scientific nature of the parameters and formula makes these research results scientific.

Table 2
Properties of skin tissue layers

Value (References) Parameters	Stratum corneum	Epidermis	Dermis	Subcutaneous fat
Thermal expansion coefficient (α)	1 (Assumption)	1 (Assumption)	1 (Assumption)	1 (Assumption)
Poisson's ratio (ν)	0.48 [19]	0.48 [19]	0.48 [19]	0.48 [19]
Young's modulus (MPa)	1998.0 [20]	102.0 [20]	10.2 [20]	0.0102 [20]
Skin density (kg/m^3)	1500.0 [21]	1190.0 [21]	1116.0 [21]	971.0 [21]
Skin thermal conductivity (W/m K)	0.235	0.235 [22]	0.445 [22]	0.185 [15]
Skin specific heat (J/kg K)	3600.0	3600.0 [15]	3300.0 [15]	2700.0 [15]
Metabolic heat generation (W/m^3)	368.1	368.1 [23]	368.1 [23]	368.3 [23]
Thickness (m)	0.00002 (Assumption)	0.00008 (Assumption)	0.0015 [24]	0.0044 (Assumption)

Table 3
Thermophysical properties of blood

Parameters	Value
Blood density(kg/m^3)	1060.0 [22]
Blood specific heat(J/kg K)	3770.0 [25]
Blood perfusion rates(ml/ml/s)	0.025 (Assumption)
Arterial blood Temperature(K)	310.15
Core temperature(K)	310.15

Results

We calculated the thermal responds of skin tissue using the FEM software COMSOL based on coupling the data obtained from the bioheat transfer.

Tonification analysis

The skin is initially kept at constant temperature. At $t = 0$, the skin surface, initially at normal temperature, is suddenly taken into contact with a hot source of burning temperature generated by tonification. According to tonification method, after 20s, the hot source is removed. Then, make the temperature keep the one at 20s for 5 seconds. Then the temperature fields are obtained by using FEM, which are subsequently used to calculate the corresponding thermal damage and thermal stress.

The calculate temperature distribution in skin tissue is plotted in Fig. 6(a), which shows that the temperature decreased exponentially along the skin depth, with a sudden decrease at the Dermis-fat interface due to the large difference between the absorption coefficients of the dermis and fat. And the temperature histories at the ED interface was shown in Fig. 6(b). The temperatures at the ED (TED) interface increase quickly after the application of the data of burning temperature. Upon temperature peak, TED decreases instantly, whereas TED decreases slowly after 20s.

Figure 7(a) plotted the corresponding thermal damage distributions along the skin depth, which was similar to that temperature. The thermal damage at the ED interface increased almost linearly during the temperature raring, as shown in Fig. 7(b). Once after the peak temperature, the thermal damage changes little, for thermal damage is a process of accumulation.

The corresponding thermal stress fields were presented along the skin depth in Fig. 8(a), which was shown that the stratum corneum layer played an important role in the mechanical behaviors of skin. The thermal stress at ED interface varied with the change of temperature, as shown in Fig. 8(b).

Sedation analysis

The skin is initially kept at constant temperature. At $t = 0$, the skin surface, initially at normal temperature, is suddenly taken into contact with a hot source of burning temperature generated by sedation. According to sedation method, after 15s, the hot source is removed and the skin was cooled by natural convection of environmental air for 5s. Then the temperature fields are obtained by using FEM, which are subsequently used to calculate the corresponding thermal damage and thermal stress.

Figure 9(a) given the temperature distribution along the skin depth at 8s, 12s, 16s, and 22s, while the temperature history at the ED interface was presented in Fig. 9. The temperature risen abruptly comparing with tonification and the peak temperature was higher than tonification. After the peak temperature, the temperature decreased sharply due to air cooling at the skin surface in the sedation method.

The thermal damage changes little once the heating is removed. The distribution of thermal damage along the skin depth is similar to that of temperature which we used, as shown in Fig. 10(a). Thermal damage at the ED interface increases almost linearly during temperature rising, but the rate is higher for the tonification, as shown in Fig. 10 (b).

The corresponding thermal stress fields were presented along the skin depth in Fig. 11 (a), and were similar with tonidication. Figure 11(b) given the thermal stress at ED interface, by comparing it and Fig. 8. (b), it can be seen that thermal stress due to sedation is larger than that due to tonification. Also, the

thermal stress is attributed to the different cooling methods used in sedation and tonification, where active cooling is often applied in sedation.

Experiment Summary

According to the above-mentioned analysis, three points have been worked out as follows:

First, for thermal transfer, as the Fig. 6(b) and Fig. 9(b) shows, the peak temperature in ED interface of sedation is higher than that of tonification. The threshold of the sensor cells for temperature pain is 43°C, so sedation has larger stimulus to skin tissue than tonification.

Second, for thermal damage, as the Fig. 7 and Fig. 10 shows, the damage caused by sedation is larger than that by tonification. So, sedation has larger stimulus to skin tissue than tonification.

Third, for thermal stress, as the Fig. 8(b) and Fig. 11(b) shows, thermal stress in ED interface caused by sedation becomes much larger than that by tonification. The mean mechanical threshold of the nociceptors in the skin is in the range of about 0–0.6 MPa [16], so sedation has larger stimulus to skin tissue than tonification.

Thus, in view of analysis above, the pain stimulation generated by sedation is much larger than that by tonification [26], which is in accordance to ancient literatures of traditional medicine.

The study of tonification and sedation in moxibustion provides a more scientific basis for physicians by using the FEM. Therefore, it is hoped that that this study will contribute to the application of, improvements in, and standardization of, tonification and sedation.

However, this study did have several limitations. Its main limitation is the assumption that the skin-tissue properties are constant. Collagen is the major component of the skin, and its thermal and mechanical properties vary with temperature. However, there have been relatively few studies regarding these changes, which limit the research on moxibustion treatment significantly. Moreover, Nishitani has suggested that other biochemical responses, such as chemical stimuli, are generated during moxibustion treatment [27].

Conclusion

The purpose of this paper was to use mathematical method to study the skin tissue produced by tonification and sedation of direct moxibustion. And the present research results shows that skin thermomechanical behavior is different influenced by tonification and sedation. Therefore, it is necessary to consider the biothermomechanical behavior such as was done in this study, before attempting to improve moxibustion and developing a moxa system using high-technology methods. Last but not least, these research results can be the foundation for researching moxibustion by using computational bioengineering, such as bio-signal generated by moxibustion. With a mathematical model, the

biothermomechanics caused by direct moxibustion can be understood and used to further develop the tool of moxibustion.

Abbreviations

FEM

finite element method; ED:epidermis-dermis; TED:temperatures at the ED.

Declarations

Ethics approval and consent to participate

Not applicable

Consent to publish

All authors read and approved the final version of the article accepted for publication.

Availability of data and materials

Not applicable

Competing interests

The authors declared no potential conflicts of interest with respect to the research, authorship, and/or publication of this article.

Funding

The author(s) received no financial support for the research, authorship, and/or publication of this article.

Authors' contributions

M.L. drafted the article. S.K. and S.L. made substantial contributions to the design of the work and critically revised the manuscript.

Acknowledgements

Not applicable.

Ethics approval and consent to participate

Not applicable.

Competing interests

The authors declare that they have no competing interests.

References

1. Zhu DPQ. The role of moxibustion in Traditional Chinese acupuncture. *Am J Acupunct.* 1984;12(2):125–32.
2. National University of Oriental Medicine. *Acupuncture*, 2nd ed. Seoul: Jipmoondang Press; 1988.
3. Kang S. *Classical Acupuncture and Moxibustion*. Seoul: Iljungsa Press; 2000.
4. Zhang Y, Geng J. *Chinese Acupuncture and Moxibustion*. Beijing: People's Medical Publishing House; 1989.
5. Litscher G. Bioengineering assessment of acupuncture, part 8: Innovative moxibustion. *Crit Rev Biomed Eng.* 2010;38(2):117–26. <https://doi/10.1615/CritRevBiomedEng.v38.i2.10>.
6. Werjie Y. Chapter 3. The Explanation of Huangdi Neijing Linggui. Seoul: Daseong Culture Press; 1990:155–156.
7. Seong-Tack I, Kyung-Ho K, Kap-Sung. K. A study of physical characteristics of moxibustion. *J Korean Acupunct Moxibustion Soc.* 1994;11(1):327–36.
8. Lee G-M, Lee GM, Hwang Y-J. Experimental study on the thermodynamic characteristics of commercial small-size moxa combustion. *J Korean Acupunct Moxibustion Soc.* 2002;18(6):171–87.
9. Geon-Mok L, Kil-soong L, Seung-Hun L, et al. The study of standardization plan and usefulness of moxa combustion. *J Korean Acupunct Moxibustion Soc.* 2003;20(6):65.
10. Chen SS, Wright NT, Humphrey JD. Phenomenological evolution equations for heat-induced shrinkage of a collagenous tissue. *IEEE Trans Biomed Eng.* 1998;45(10):1234–40. <https://doi/10.1109/10.720201>.
11. Ebling F, Eady R, Leigh I. Anatomy and organization of human skin. In: Champion RH, Burrington JL, Ebling FJG, editors. *Textbook of Dermatology*. New York: Blackwell Scientific; 1992. p. 3160.
12. Tregear RT. *Physical Functions of Skin*. New York: Academic Press; 1966.
13. Pennes HH. Analysis of tissue and arterial blood temperatures in the resting human forearm. *J Appl Physiol.* 1948;1(2):93–122. <https://doi/10.1152/jappl.1948.1.2.93>.
14. Moritz AR, Henriques FC. Study of thermal injuries, II: the relative importance of time and surface temperature in causation of cutaneous burns. *Am J Pathol.* 1947;23(5):695–720.
15. Henriques FC, Moritz AR. Studies of thermal injury: 1. the conduction of heat to and through skin and the temperatures attained therein. a theoretical and an experimental investigation. *Am J Pathol.* 1947;23(4):531–49.
16. James NC, Richard AM. *Neurobiology of Nociceptors*. Oxford: Oxford University Press; 1996.
17. Pepper DW, Herrich JC. *The Finite Element Method: Basic Concepts and Applications*. London: Taylor & Francis; 1992.

18. Liu M, Kauh SK, Lim S. A study of direct moxibustion using mathematical methods. *Comput Methods in Biomech Biomed Engin.* 2012;15(4):383–91. <https://doi/10.1080/10255842.2010.538387>.
19. Delalleau A, Josse G, Lagarde JM, Zahouani H, Bergheau JM. Characterization of the mechanical properties of skin by inverse analysis combined with the indentation test. *J Biomech.* 2006;39(9):1603–10. <https://doi/10.1016/j.jbiomech.2005.05.001>.
20. Hendriks FM, Brokken D, Oomens CW, Bader DL, Baaijens FP. The relative contributions of different skin layers to the mechanical behavior of human skin in vivo using suction experiments. *Med Eng Phys.* 2006;28(3):259–66. <https://doi/10.1016/j.medengphy.2005.07.001>.
21. Duck FA. *Physical properties of tissue: a comprehensive reference book.* London: Academic Press; 1990.
22. Elkins W, Thomson JG. *Thermal Instrumented Manikintm: Aerotherm Division Report AD-781.* Mountain View: Acurex Corporation; 1973. p. 176.
23. Roetzel W, Xuan Y. Transient response of the human limb to an external stimulus. *Int J Heat Mass Transfer.* 1998;41(1):229–39. [https://doi/10.1016/S0017-9310\(96\)00160-3](https://doi/10.1016/S0017-9310(96)00160-3).
24. Dahan S, Lagarde JM, Turlier V, Courrech L, Mordon S. Treatment of neck lines and forehead rhytids with a nonablative 1540-nm Er: glass laser: a controlled clinical study combined with the measurement of the thickness and the mechanical properties of the skin. *Dermatol Surg.* 2004;30(6):872–9. <https://doi/10.1111/j.1524-4725.2004.30256.x>.
25. Torvi DA, Dale JD. A finite element model of skin subjected to a flash fire. *J Biomech Eng.* 1994;116(3):250–5. <https://doi/10.1115/1.2895727>.
26. Brooks J, Tracey I. From nociception to pain perception: imaging the spinal and supraspinal pathways. *J Anat.* 2005;207(1):19–33. <https://doi/10.1111/j.1469-7580.2005.00428.x>.
27. Nishitani I. *Combustion Products of Moxibustion.* The Japan Society of Acupuncture and Moxibustion.1987;37–33.

Figures



Figure 1

Direct Moxibustion

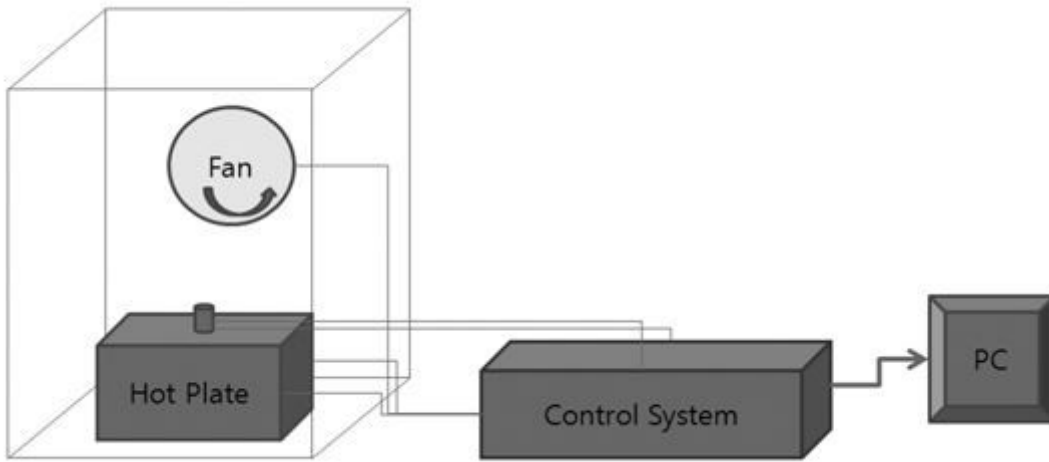


Figure 2

Temperature measurement system

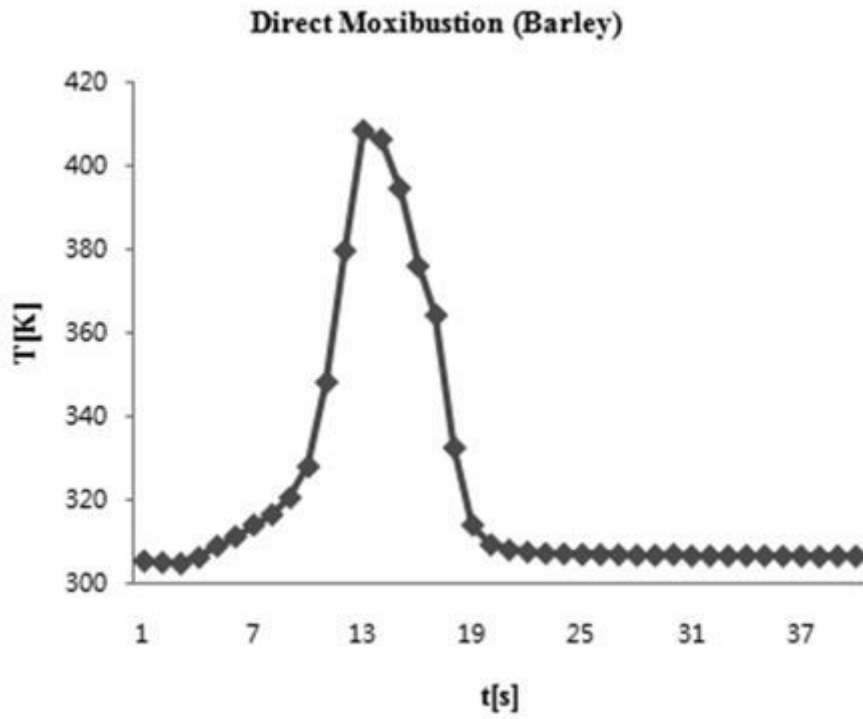


Figure 3

The temperature of direct moxibustion (barley seed) over time

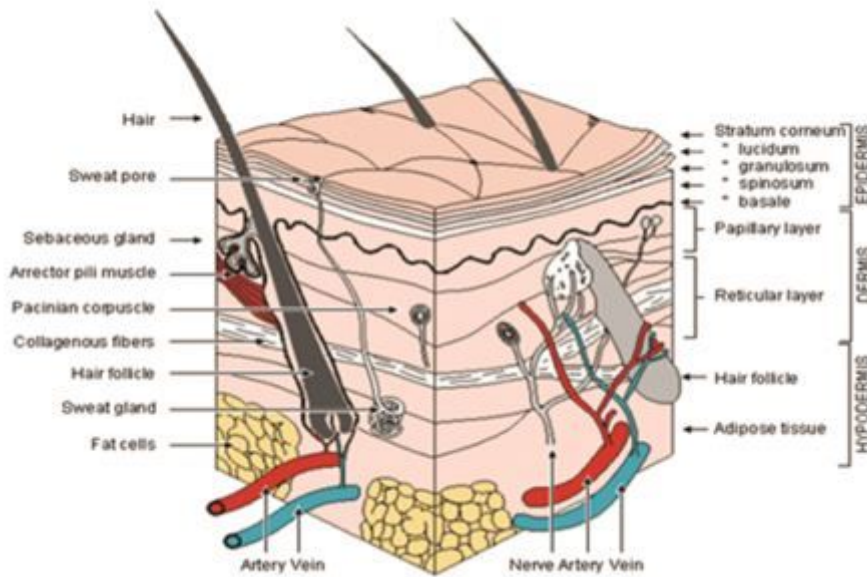


Figure 4

Section of smooth skin11

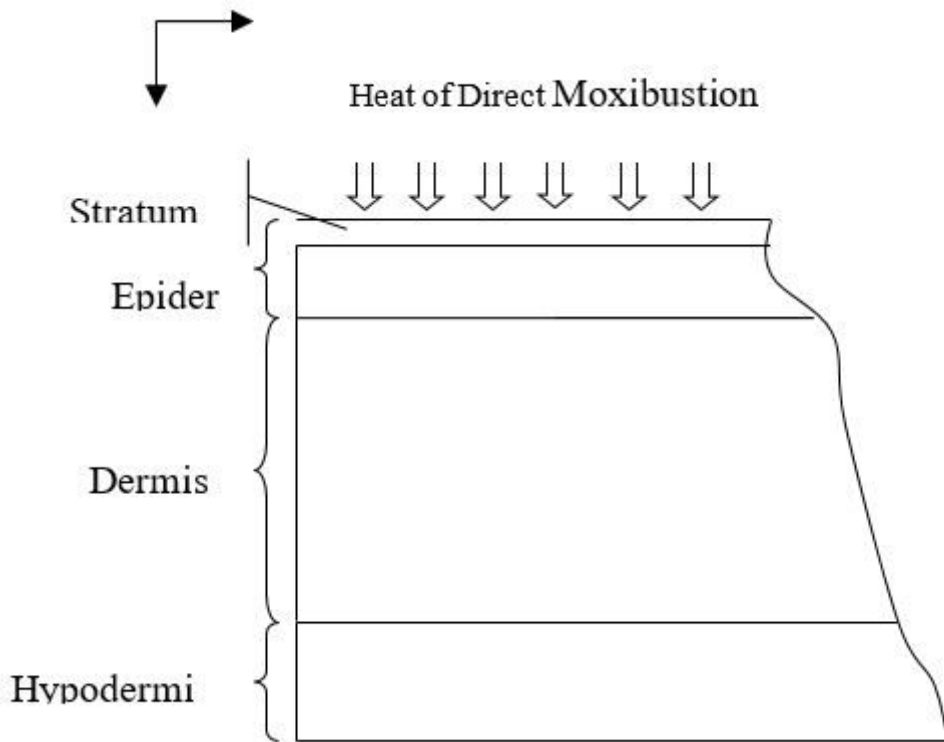


Figure 5

Ideal skin layers for direct moxibustion

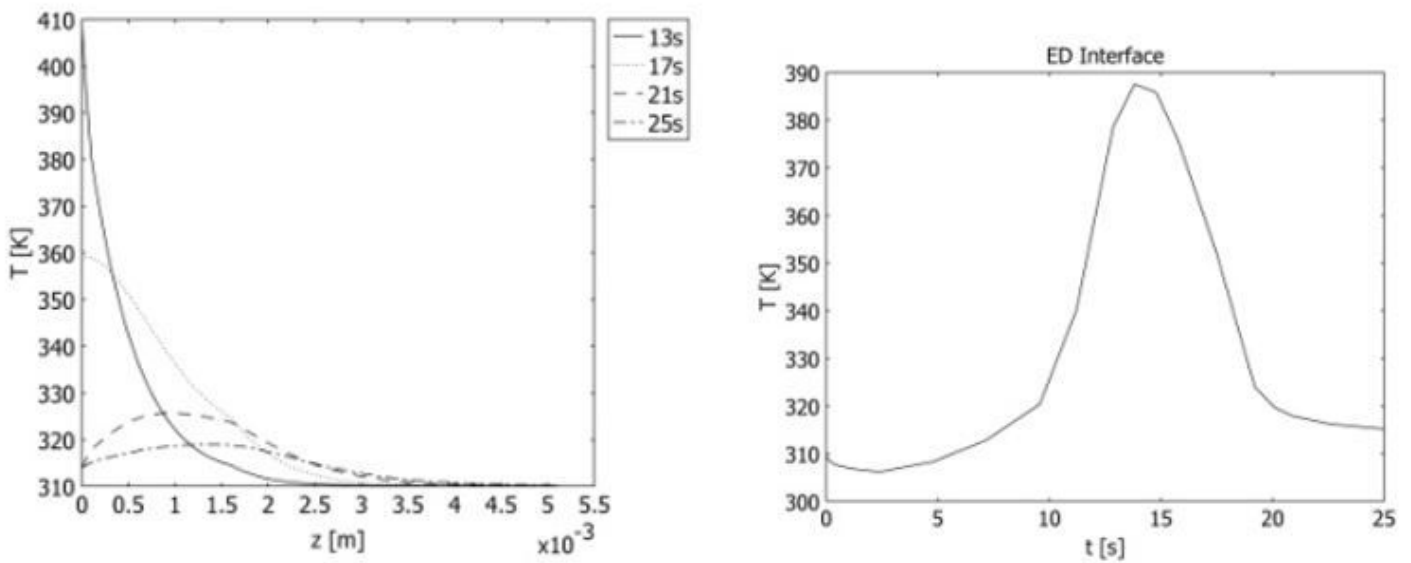


Figure 6

(a) Temperature distribution in skin at (t=10 s, 13 s, 16 s, and 20 s); (b) temperature history at the ED interface.

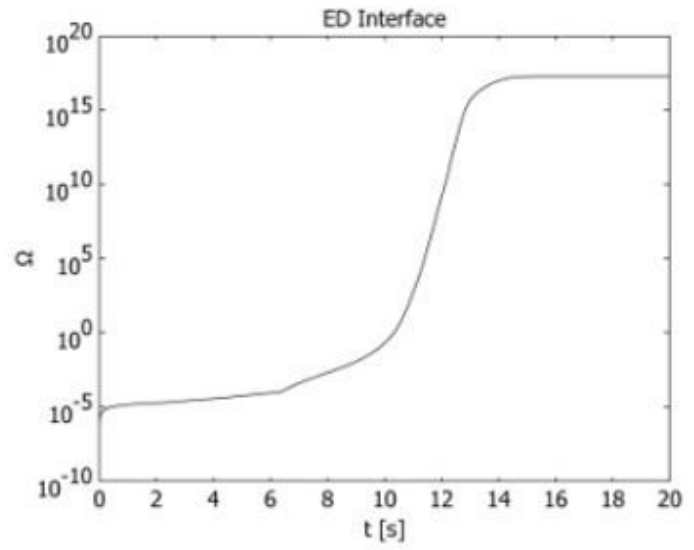
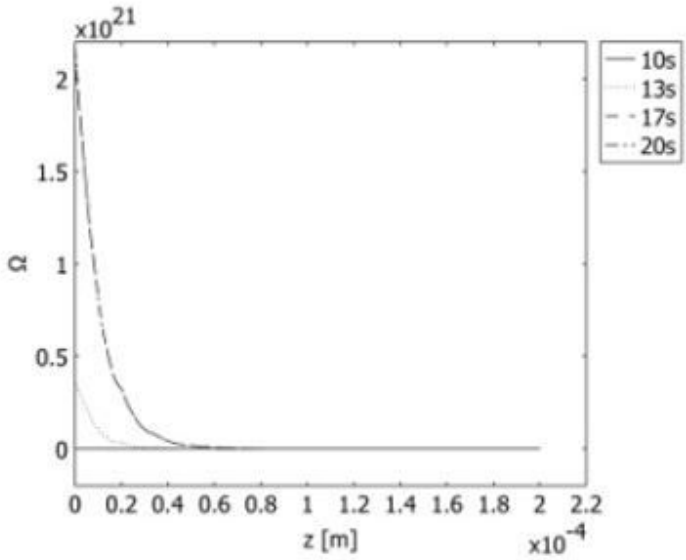


Figure 7

(a) Thermal damage distribution in skin at ($t=10$ s, 13 s, 16 s, and 20 s); (b) Thermal damage history at the ED interface.

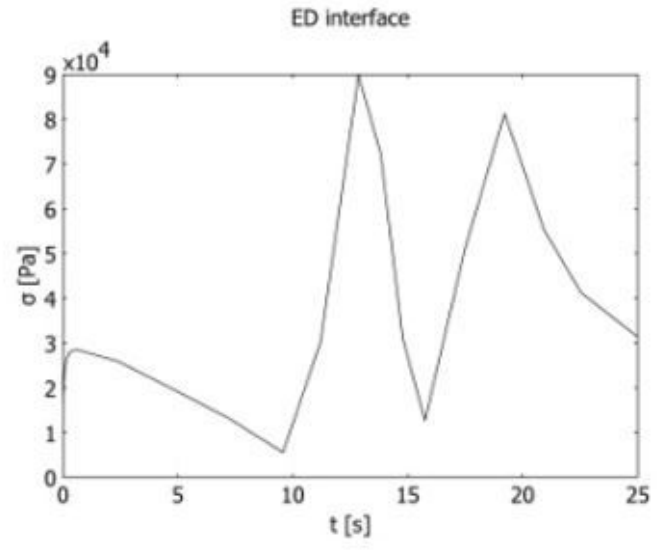
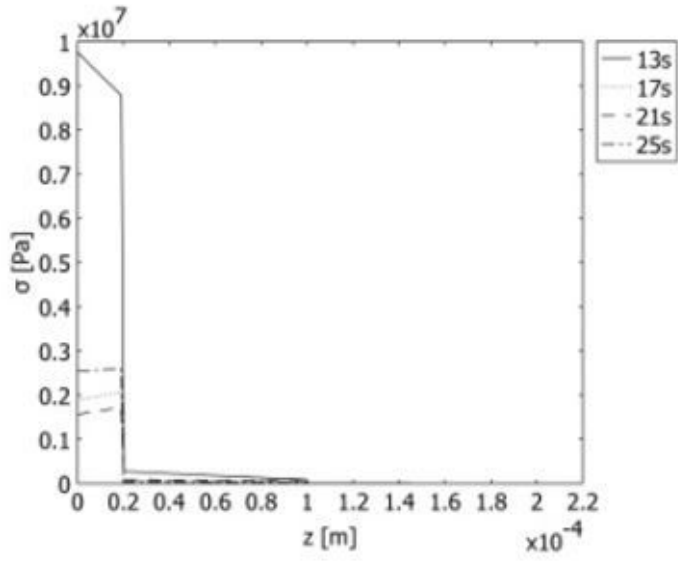


Figure 8

(a) Thermal stress distribution in skin at ($t=10$ s, 13 s, 16 s, and 20 s); (b) Thermal stress history at the ED interface.

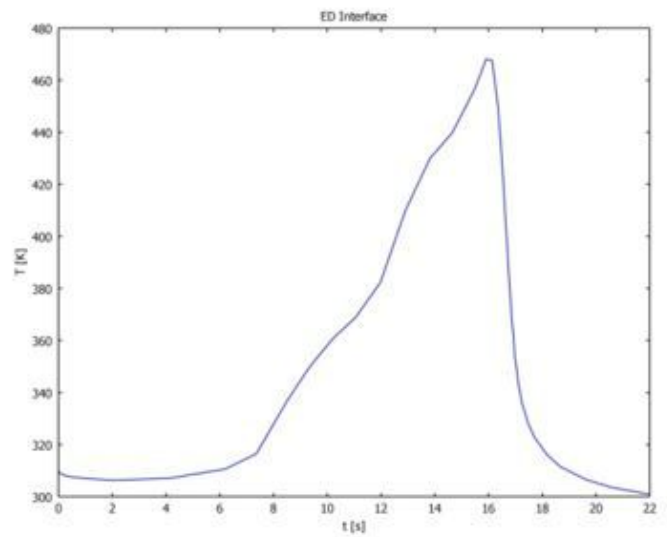
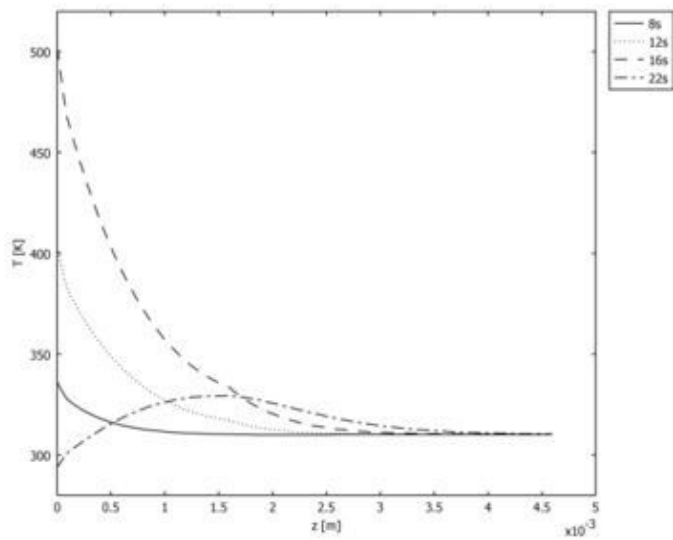


Figure 9

(a) Temperature distribution in skin at (t=8s, 12s, 16s, and 22s); (b) temperature history at the ED interface.

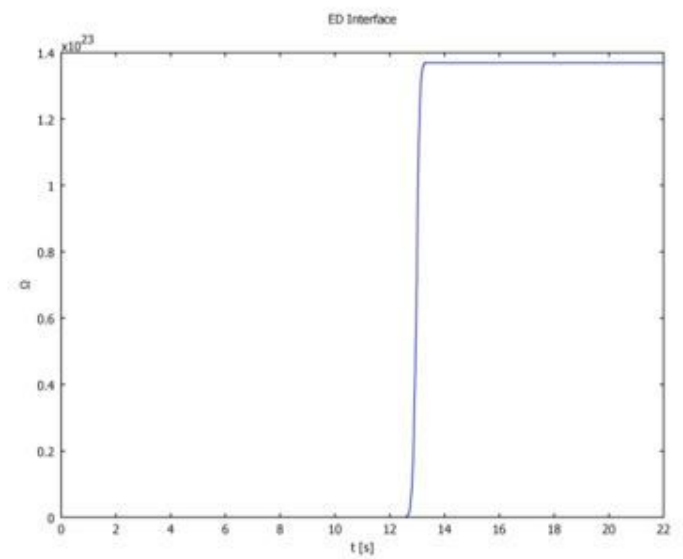
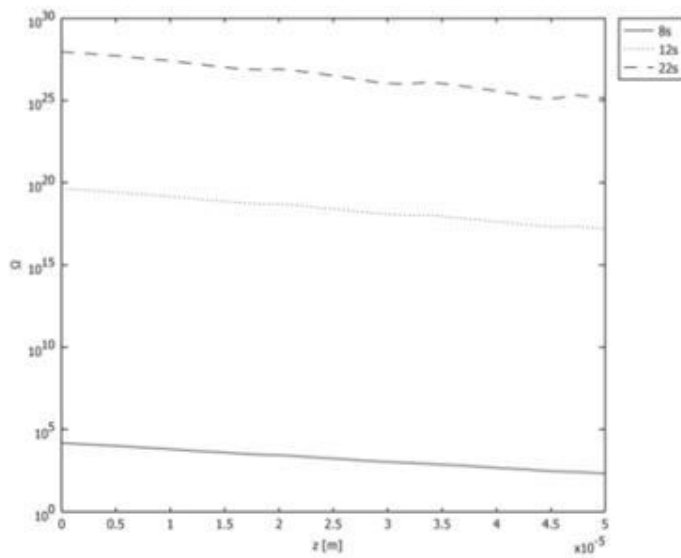


Figure 10

(a) Thermal damage distribution in skin at (t=8s, 12s, and 22s); (b) Thermal damage history at the ED interface.

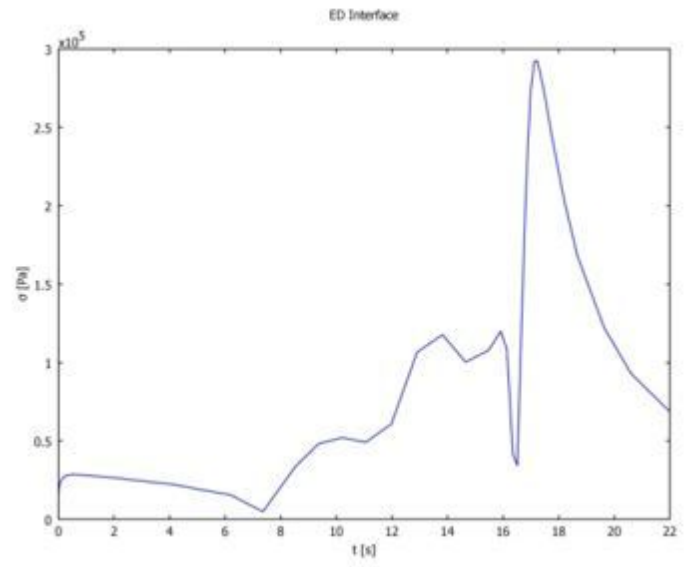
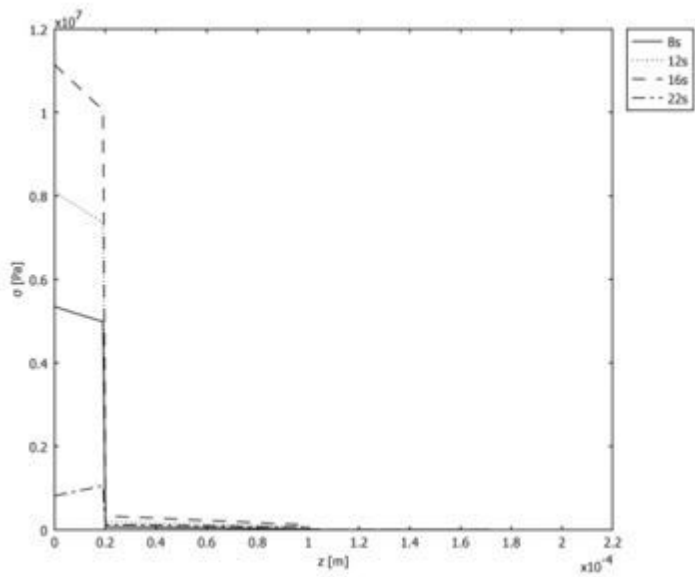


Figure 11

(a) Thermal stress distribution in skin at ($t=8$ s, 12s, 16s, and 22s); (b) Thermal stress history at the ED interface.